Available online at www.sciencedirect.com
ScienceDirect
Polymer 49 (2008) 2146–2152
polymer
www.elsevier.com/locate/polymer

Thermal expansion behavior of composites based on non-axisymmetric ellipsoidal particles

Kee-Yoon Lee [a], S.R. Hong [a], S.K. Jeoung [b], N.H. Kim [c], S.G. Lee [d], D.R. Paul [e,*]

[a] Department of Polymer Science and Engineering, Chungnam National University, Daejeon, Republic of Korea
[b] Korea Automotive Technology Institute, Chonan, Republic of Korea
[c] Hanwha L&C Corporation, Cheongwon, Republic of Korea
[d] Department of Advanced Organic Materials and Textile System Engineering, Chungnam National University, Daejeon, Republic of Korea
[e] Department of Chemical Engineering and Texas Materials Institute, University of Texas at Austin, Austin, TX 78712, United States

Received 3 December 2007; received in revised form 14 February 2008; accepted 16 February 2008
Available online 21 February 2008

Abstract

A new model for calculating the coefficients of thermal expansion, CTE, in all three coordinate directions is developed for composites containing non-axisymmetric, ellipsoidal particles, i.e., three-dimensional ellipsoids ($a_1 \neq a_2 \neq a_3$) characterized by two aspect ratios, $\rho_\alpha = a_1/a_3$ and $\rho_\beta = a_1/a_2$. The model makes use of Eshelby's equivalent tensor for the particles and utilizes the methodology from recent papers by Lee et al. The effects of the primary, ρ_α, and secondary, ρ_β, aspect ratios and filler volume fraction (0–6%) on the various CTE for nanocomposites containing aligned inclusions are demonstrated by calculations for a matrix of nylon 6 and a filler of montmorillonite single platelets. The CTE in the longitudinal direction, α_{11}, decreases, as both aspect ratios increase. The CTE in the transverse direction, α_{22}, decreases as ρ_α increases but increases as ρ_β increases. The CTE in the normal direction, α_{33}, is greater than that of the matrix and increases as ρ_α increases but decreases as ρ_β increases.

Keywords: Composites; Polymers; Thermal expansion

1. Introduction

Developing polymer-based composites and understanding their mechanical and thermal behavior in terms of the properties of the polymer matrix and the filler have been of active interest for decades [1–33]. The majority of the literature has been concerned with the mechanical properties of composites; however, thermal expansion behavior is of growing concern particularly for automotive applications where plastic and metal parts are used together [30–32]. The thermal expansion of composites depends on the elastic and thermal properties of the matrix and filler (or inclusions) plus the geometry, concentration and orientation of the filler particles.

Much of the prior literature has focused on fiber reinforcement, but with the advent of nanocomposites containing inclusions of montmorillonite-based organoclays (MMT), there is a growing interest in fillers with other shapes, like platelets [10,11]. The particle shapes in nanocomposites based on clay may be irregular with no axes of symmetry. Moreover there is a distribution of particle sizes. The objective here is to extend the recent work by Lee et al. [1,4] to develop a model for calculating the coefficients of linear thermal expansion, CTE, in all three coordinate directions for polymer composites containing aligned non-axisymmetric, ellipsoidal particles of uniform size but with no axes of symmetry characterized by two aspect ratios as illustrated in Fig. 1. Previously developed theories, including Eshelby's equivalent tensor [2], and Mori–Tanaka's average stress [3] will be used in ways illustrated in previous papers [1,4]. The effects of the aspect ratios on the CTE of nanocomposites containing aligned and well-bonded

* Corresponding author. Tel.: +1 512 471 5392; fax: +1 512 471 0542.
E-mail address: drp@che.utexas.edu (D.R. Paul).

0032-3861/$ - see front matter © 2008 Elsevier Ltd. All rights reserved.
doi:10.1016/j.polymer.2008.02.025

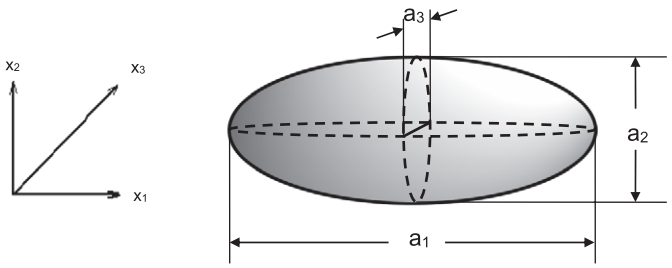

Fig. 1. Schematic of the ellipsoidal inclusions, or filler particles, characterized by two aspect ratios: a primary aspect ratio $\rho_\alpha = a_1/a_3$ and a secondary aspect ratio $\rho_\beta = a_1/a_2$. These coordinate directions are described in the text as the longitudinal (x_1), transverse (x_2), and normal (x_3) directions.

inclusions with the properties of MMT in a polymer matrix with the properties of nylon 6 are examined including the limiting cases of spherical, fiber-like and disc-like ellipsoidal shapes. The effect of exfoliated MMT platelets is quite significant even at the low loadings typical for nanocomposites. In view of this, the calculations presented here focus on the concentration range below 6 vol% of MMT or 13.7 wt%. The properties of the matrix and the filler shown in Table 1 were taken from the literature [6,10].

2. Background

Many sophisticated analytical or numerical analyses of composite behavior based on applied mechanics have been reported in the literature; however, the work of Eshelby [2], Hill [11] and Mori and Tanaka [3] on self-consistent approaches to heterogeneous materials are of particular use here. A brief summary of some of the prior theoretical and experimental efforts relevant to the current objective is given below.

Halpin and Tsai [12], Schapery [13], Wakashima et al. [14], Takao and Taya [15], Chow [7–9] and Tandon and Weng [6] developed analytical methodologies to compute the effective thermal and mechanical properties of composite materials consisting of a matrix and aligned inclusions as a function of particle concentration. Pierard et al. [16] and Doghri and Tinel [17] proposed mean-field homogenization models using Eshelby-based techniques for thermo-elastic composites, while Li [18] used direct homogenization schemes with an effective-medium-field micromechanics approximation. Lusti et al. [19], Dray et al. [20], and Hbaieb et al. [21] have used finite-element based numerical approaches for nanocomposites and short fiber reinforced composites. Glavche et al. [22], and Alagar et al. [23] studied the coefficients of thermal expansion of epoxy compositions containing various fillers as a function of temperature and intermolecular adhesion of the epoxy resin with the filler. Bowles and Tompkins [5] compared the predictions from several analyses for the CTE of composites containing carbon or graphite fibers in two directions with experimental data.

Yoon et al. [10] and Yalcin and Cakmak [24] observed by transmission electron microscopy and atomic force microscopy, respectively, that particles of MMT have a complex distribution of shapes. These examples clearly indicate that, in general, to describe such particles requires two aspect ratios. Yoon et al. [10] and Fornes and Paul [25,26] reported experimental data on the CTE and modulus of nanocomposites based on these materials. Lee et al. [31] and Ellis and D'Angelo [32] have reported experimental relationships between the CTE behavior of nanocomposites based on thermoplastic olefin (TPO) materials and their morphology. Wei et al. [33] and Zhang and Wang [34] investigated the CTE of polymer composites based on carbon nanotubes by means of thermo-elastic theory and conventional models.

In this paper, a model is developed for predicting the effects of particle geometry on the linear CTE of composites in all three coordinate directions, α_{ii}, plus the volumetric CTE, γ, relative to that of the matrix, α_m, i.e., α_{11}/α_m, α_{22}/α_m, α_{33}/α_m, and $\gamma/3\alpha_m$, using procedures described in previous papers [1,4], for polymer nanocomposites containing aligned ellipsoidal filler particles ($a_1 \neq a_2 \neq a_3$) characterized by two aspect ratios defined as $\rho_\alpha = a_1/a_3$ and $\rho_\beta = a_1/a_2$, see Fig. 1.

Table 1
Material properties of the matrix (nylon 6) and the filler (montmorillonite platelets, MMT) used in the calculations

	Density (g/cm^3)	Modulus (GPa)		Linear CTE $\times 10^6$ (K^{-1})		Poisson's ratio	
Nylon 6	1.14	E_m	2.75	α_m	85.0	ν_m	0.33
MMT	2.83	E_f	178.0	α_f	1.67	ν_f	0.20

The material constants were taken from Refs. [6,10].

3. Basic theory

For composite materials, the average strain over an adequate system volume $\overline{\varepsilon}_{ii}$ is not equal to the strain of the polymer matrix ε_{ii}^m due to the effect of the inclusions. This problem has to do with the perturbation strains of the matrix and filler, which are the differences between the local strain and the average strain, and the corresponding average perturbed stresses for the matrix and for the filler. As the temperature changes in the absence of any external stress, the external strain, $\overline{\varepsilon}_{ij}$, which is expressed by the expansional internal strain, can be related to the coefficients of the linear thermal expansion $(\alpha_m)_{ii}$ of the polymer matrix as follows [1]

$$\frac{\overline{\varepsilon_{ij}}\cdot\delta_{ij}}{\varepsilon_{ii}^m} = \frac{\alpha_{ij}\cdot\delta_{ij}}{(\alpha_m)_{ii}} = 1 + \phi\frac{\varepsilon_{ij}^t\cdot\delta_{ij}}{\varepsilon_{ii}^m} \tag{1}$$

where ε_{ii}^m is the strain of the polymer matrix, α_{ij} is the coefficient of linear thermal expansion of the composite material, ε_{ij}^t is the equivalent transformation strain of the ellipsoidal shaped inclusions [1,6] without external volume-average stress ($\overline{\boldsymbol{\sigma}} = 0$), δ_{ij} is the Kronecker delta, and ϕ is the volume fraction of the inclusions. Note that the CTE of composites where the matrix is anisotropic, which is frequently the case for parts formed by injection molding [10] or other high shear stress processing, can be calculated by using anisotropic terms for $(\alpha_m)_{ii}$ in the current model.

With the assumption that the polymer matrix is isotropic, its coefficients of linear thermal expansion are $(\alpha_m)_{11} = (\alpha_m)_{22} = (\alpha_m)_{33} = \alpha_m$ and the strains of the polymer matrix are $\boldsymbol{\varepsilon}^m_{11} = \boldsymbol{\varepsilon}^m_{22} = \boldsymbol{\varepsilon}^m_{33} = \boldsymbol{\varepsilon}^m$, so Eq. (1) becomes

$$\frac{\overline{\varepsilon_{ij}}\cdot\delta_{ij}}{\varepsilon^m} = \frac{\alpha_{ij}\cdot\delta_{ij}}{\alpha_m} = 1 + \phi\frac{\varepsilon^t_{ij}\cdot\delta_{ij}}{\varepsilon^m} \tag{2}$$

Using the concept of $A^t_{ij} = \varepsilon^t_{ij}/(\alpha_m)_{ii}\Delta T$, corresponding to the transformation strain tensor, ε^t_{ij} given by Eshelby's equivalent principle [2], this result can be expressed as

$$\frac{\alpha_{ii}}{(\alpha_m)_{ii}} = 1 + \phi\frac{\varepsilon^t_{ij}\cdot\delta_{ij}}{(\alpha_m)_{ii}\Delta T} = 1 + \phi A^t_{ij}\cdot\delta_{ij} \tag{3}$$

Using Eshelby's superposition principles [2] and the Lamé constants, the governing equation can be expressed as

$$\left(C^f_{ijkl} - C^m_{ijkl}\right)\left[1 + (1-\phi)S_{klmn}A^t_{ij} + \phi A^t_{ij}\right] + C^m_{ijkl}\,A^t_{ij} = 0 \tag{4}$$

The relation between the unknown A^t_{ij} and known parameters, such as ε^m_{kl}, ϕ, C^m_{ijkl}, C^f_{ijkl} and S_{klmn} can be expressed by the simple matrix M_{IJ} by using a simplified form of Eq. (4) made possible by the fact that the coefficients of linear thermal expansion α_{ij} have physical meaning only in the x_1, x_2, and x_3 coordinate directions. This relationship is

$$M_{IJ}A^t_I = M_{I4}, \quad (I \text{ and } J = 1, 2 \text{ and } 3) \tag{5}$$

$$\begin{bmatrix} M_{11} & M_{12} & M_{13} \\ M_{21} & M_{22} & M_{23} \\ M_{31} & M_{32} & M_{33} \end{bmatrix}\begin{bmatrix} A^t_1 \\ A^t_2 \\ A^t_3 \end{bmatrix} = \begin{bmatrix} M_{14} \\ M_{24} \\ M_{34} \end{bmatrix} \tag{6}$$

where the simplified C^m_{IJ}, Eshelby's tensor S_{klmn} for inclusions with an ellipsoid-like shape, and M_{IJ} are all explained by Lee and Paul [4] except for M_{I4} which is given by

$$M_{I4} = -\varepsilon^m_1(D_1 + 2), \quad (I = 1, 2 \text{ and } 3) \tag{7}$$

The components of the three by three matrix, M_{IJ}, consist of known parameters that can be used to calculate the ratio of the equivalent transformation strain of the linear thermal expansion matrix A^t_I by using an appropriate numerical method [35]. Finally, the coefficients of linear thermal expansion for the composite can be calculated from Eqs. (3), (6) and (7).

The volumetric or bulk coefficient of thermal expansion of the polymer matrix, γ_m, and of the composite, γ, can be obtained by summation of the linear CTE as follows

$$\gamma_m = (\alpha_m)_{11} + (\alpha_m)_{22} + (\alpha_m)_{33} \tag{8}$$

$$\gamma = \alpha_{11} + \alpha_{22} + \alpha_{33} \tag{9}$$

With the assumption that the polymer matrix is isotropic, the volumetric thermal expansion coefficient of the matrix is given by $\gamma_m = 3\alpha_m$.

4. Numerical results and discussion

The effects of the aspect ratios and the volume fraction of ellipsoidal inclusions on the CTE are illustrated here for nanocomposites based on MMT in a nylon 6 matrix. The shape of MMT particles can be more complex but are approximated here as ellipsoidal particles as illustrated in Fig. 1, where we take $a_1 > a_2 > a_3$; such particles are geometrically characterized by a primary aspect ratio, $\rho_\alpha = a_1/a_3$, and a secondary aspect ratio, $\rho_\beta = a_1/a_2$. The material properties of the MMT filler and the glassy polyamide matrix are listed in Table 1 [6,10]. In what follows, the polymer matrix is assumed to be isotropic; however, the current model can handle composites where the matrix is anisotropic.

Normalized linear CTE in the longitudinal direction, α_{11}/α_m, in the transverse direction, α_{22}/α_m, in the normal direction, α_{33}/α_m, and the normalized bulk CTE, $\gamma/3\alpha_m$, are shown in Fig. 2 as a function of the volume fraction of filler ϕ, from 0 to 0.06, for cases where the primary aspect ratio $\rho_\alpha = 10$ and 100 while the secondary aspect ratio $\rho_\beta = 1$, 4, or ρ_α.

In Fig. 2(a), the normalized CTE in the longitudinal direction, α_{11}/α_m, monotonically decreases for given primary and secondary aspect ratios as filler content ϕ increases due to the mechanical constraint that the high modulus filler provides against expansion of the matrix, which has a lower modulus but a higher thermal expansion coefficient. The decrease in CTE in this direction is less for disc-shaped inclusions ($\rho_\beta = 1$, $a_1 = a_2$) than for fiber-shaped inclusions ($\rho_\alpha = \rho_\beta$, $a_2 = a_3$). The examples for $\rho_\beta = 4$ lie in between these limits. As expected, the larger the primary aspect ratio, the greater the effects on CTE are. The mathematical form of the current model leads to numerical difficulties for calculations in the exact limit of disc ($a_1 = a_2$ or $\rho_\beta = 1$) and fiber ($a_2 = a_3$ or $\rho_\alpha = \rho_\beta$) shapes; however, the results do properly extrapolate to the limits for these axisymmetric ellipsoidal particles, see Lee et al. [1,4].

Fig. 2(b) shows that the normalized CTE in the transverse direction, α_{22}/α_m, decreases or remains nearly constant as the volume fraction of filler ϕ increases for shapes with some disc-like character; however, for fiber shapes, $\rho_\alpha = \rho_\beta$, the CTE in this direction increases. Thus, α_{22}/α_m increases as the secondary aspect ratio, ρ_β, increases, i.e., as the inclusions become more fiber-like. Since fibers constrain expansion of the matrix mainly in the x_1 direction, whereas discs constrain the matrix equally in the x_1 and the x_2 directions, it is understandable that α_{22}/α_m increases as the particles become more like fibers. Fiber-shaped inclusions, which have the maximum secondary aspect ratio for a given primary aspect ratio, show the largest thermal expansion in the transverse direction, α_{22}/α_m, as seen in Fig. 2(b).

Fig. 2(c) shows the normalized CTE in the normal direction, α_{33}/α_m, initially increases for the primary and secondary aspect ratios shown as the volume fraction of filler, ϕ, increases. In all cases, α_{33}/α_m increases as ρ_α increases but decreases as ρ_β increases. Disc-shaped inclusions show a greater increase in α_{33}/α_m than do fiber-shaped particles. When $\rho_\alpha = 100$, the case of $\rho_\beta = 4$ falls between the disc and fiber limits; however, this is not so clear for the case of $\rho_\alpha = 10$. It is

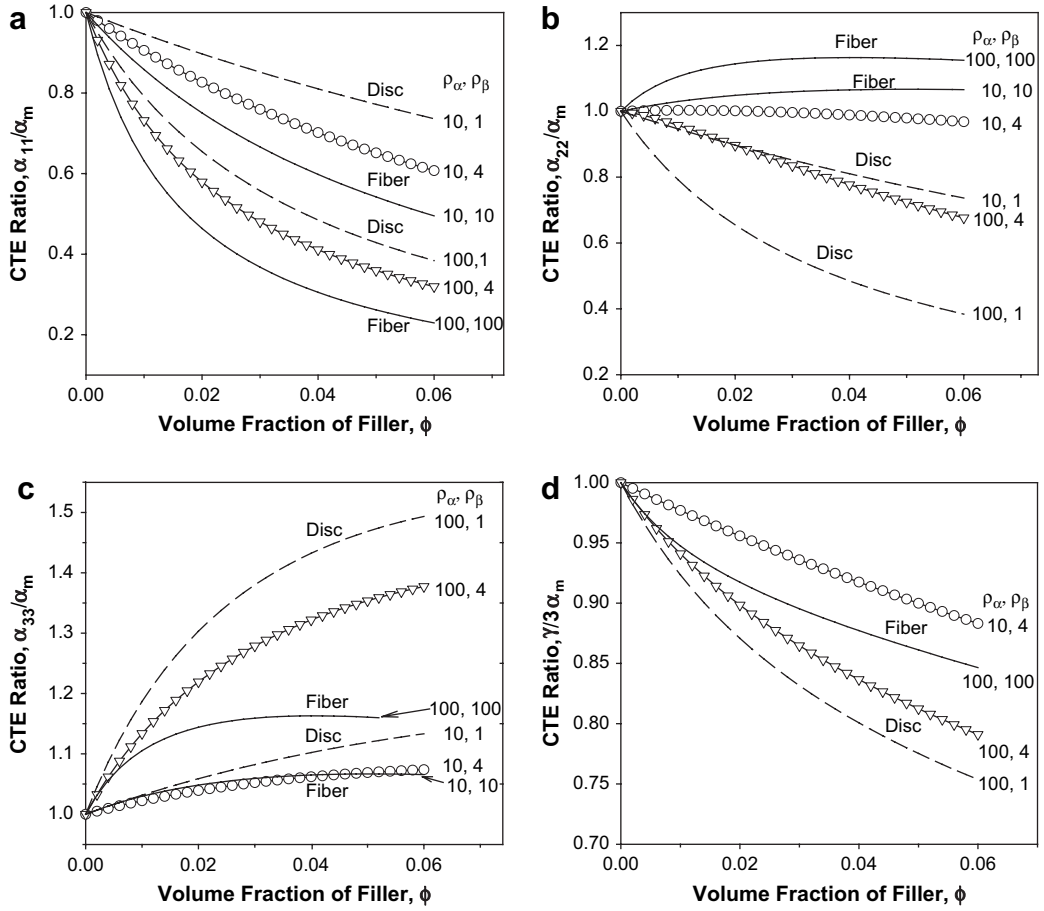

Fig. 2. Normalized coefficients of linear thermal expansion in the (a) longitudinal direction, α_{11}/α_m, in the (b) transverse direction, α_{22}/α_m, and in the (c) normal direction, α_{33}/α_m, and the (d) bulk coefficient of thermal expansion, $\gamma/3\alpha_m$, of composites as a function of the volume fraction of filler, assumed to have the properties of montmorillonite or MMT, for given primary aspect ratios $\rho_\alpha = 10$ and 100 and secondary aspect ratios $\rho_\beta = 1$, 4 and ρ_α. The matrix is assumed to have the properties of nylon 6.

important to reiterate that for fibers $\alpha_{22}/\alpha_m = \alpha_{33}/\alpha_m$, due to symmetry about the x_1 axis, while for discs $\alpha_{22}/\alpha_m = \alpha_{11}/\alpha_m$ due to the symmetry about the x_3 axis.

As seen in Fig. 2(d), the normalized bulk CTE, $\gamma/3\alpha_m$, decreases as the volume fraction of filler, ϕ, increases for all values of the primary and secondary aspect ratios. The bulk expansion decreases as ρ_α increases but increases as ρ_β increases. Discs cause a greater reduction in volumetric expansion than fibers. The three linear CTEs show different trends caused by mechanical constraint in some directions and squeezing out in other directions; however, in computing the bulk expansion coefficient from the sum of the linear CTE there is a tendency for cancellation of these positive and negative effects. Thus, $\gamma/3\alpha_m$ shows much less effect from adding inclusions than do the linear coefficients.

In the remaining examples, the effect of the particle aspect ratios on the various thermal expansion coefficients, at a fixed filler volume fraction, $\phi = 0.015$, will be demonstrated with particular emphasis on the cases in between fibers and discs by varying ρ_β. Normalized linear CTE are shown in Fig. 3 as a function of the secondary aspect ratio, ρ_β, for a given primary aspect ratio, $\rho_\alpha = 100$, and given volume fraction of

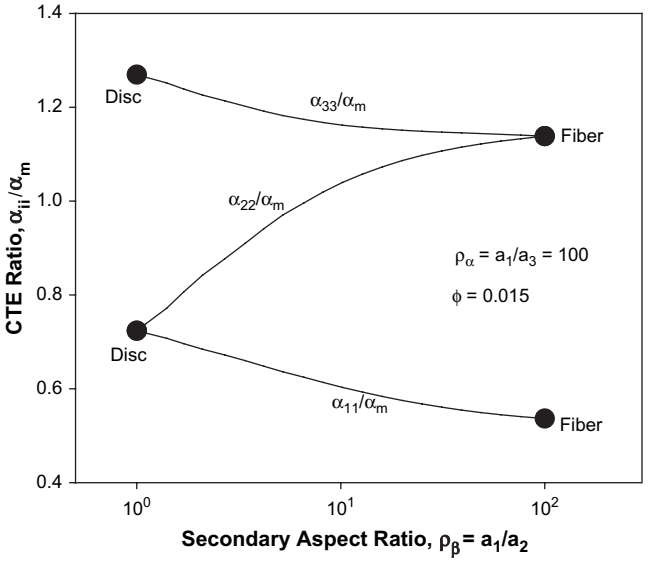

Fig. 3. Normalized coefficients of linear thermal expansion in the longitudinal direction, α_{11}/α_m, in the transverse direction, α_{22}/α_m, and in the normal direction, α_{33}/α_m, as a function of the secondary aspect ratio ρ_β for a given primary aspect ratio $\rho_\alpha = 100$ and a given volume fraction of MMT filler of $\phi = 0.015$.

filler, $\phi = 0.015$. The effects of the secondary aspect ratio on the linear CTE in various directions [1] are clearly seen here even for this low loading of MMT. The longitudinal CTE, α_{11}/α_m, smoothly changes from the value for a fiber-shaped inclusion to that of a disc-shaped one as ρ_β decreases from 100 to 1. For the disc-shape, where $a_1 = a_2$ and $\rho_\beta = 1$, $\alpha_{11}/\alpha_m = \alpha_{22}/\alpha_m$. The transverse CTE, α_{22}/α_m, increases from the value of a disc-shaped inclusion to that of a fiber-shaped one as ρ_β increases from 1 to 100. For the fiber-shaped inclusion where $a_2 = a_3$ and $\rho_\alpha = \rho_\beta$, $\alpha_{22}/\alpha_m = \alpha_{33}/\alpha_m$. The normal direction CTE, α_{33}/α_m, goes smoothly from the value of a disc-shaped inclusion to that of a fiber shape as ρ_β decreases from 100 to 1. The effects of the secondary aspect ratio will be addressed more fully later.

In Fig. 4, the linear CTE ratios, are shown as a function of the primary aspect ratio ρ_α for a given volume fraction $\phi = 0.015$ and a secondary aspect ratio $\rho_\beta = 4$ by the solid lines and compared with those for disc-shaped (short dashes) and fiber-shaped (long dashes) inclusions. The CTE ratio in the longitudinal direction, α_{11}/α_m, monotonically decreases as ρ_α increases; it is greater than that for fiber-shaped inclusions and less than that for the disc-shaped particles, due to the differences in longitudinal constraint. As ρ_α increases to values of the order of 1000, α_{11}/α_m approaches a limiting value almost like that for the disc-shaped inclusion. In the limit of very high aspect ratios, the model correctly converges to the limit of a simple parallel model. As ρ_α increases, the CTE ratio in the transverse direction, α_{22}/α_m, decreases like α_{11}/α_m, but not as strongly until high aspect ratios are reached; its value at given aspect ratio is greater than that for the corresponding disc-shaped inclusion but less than that for the fiber shape. At high values of ρ_α, α_{22}/α_m approaches a limiting value like α_{11}/α_m for similar reasons. The CTE ratio in the normal direction, α_{33}/α_m, increases as ρ_α increases, because of the restraint caused by the inclusion in the x_1 and, to some extent, the x_2 directions which squeezes the composite outwardly in the x_3 direction. For a given ρ_α, α_{33}/α_m is less than that for the disc-shaped inclusion but approaches this limiting value as ρ_α becomes vary large. For $\rho_\alpha < 10$, all of the linear CTEs are not much different from that of the matrix at this low loading of filler, $\phi = 0.015$.

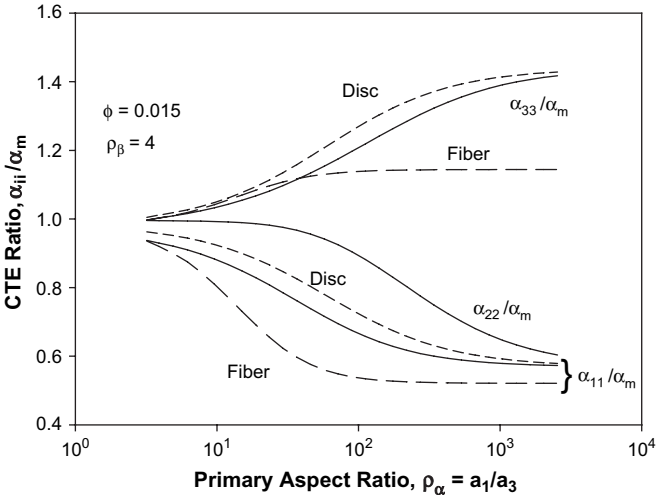

Fig. 4. Normalized coefficients of linear thermal expansion in the longitudinal direction, α_{11}/α_m, in the transverse direction, α_{22}/α_m, and in the normal direction, α_{33}/α_m, as a function of the primary aspect ratio ρ_α for a given volume fraction $\phi = 0.015$ and a secondary aspect ratio $\rho_\beta = 4$. The results are also compared with the limiting cases of the disc- and fiber-shaped inclusions.

Fig. 5 shows the various normalized CTEs as functions of the primary aspect ratio, ρ_α, for a given volume fraction, $\phi = 0.015$, and specific secondary aspect ratios such as $\rho_\beta = 2, 4, 8$ and 16; the limits for disc- and fiber-shaped inclusions are also shown. As ρ_α increases, expansion in the longitudinal direction, α_{11}/α_m, decreases for all secondary aspect ratios, and for the fiber- and disc-shaped models as seen in Fig. 5(a). As ρ_β increases for a given ρ_α, α_{11}/α_m decreases from the upper limit of the disc-shaped inclusion to the lower limit of the fiber-shaped one. The effect of the constraint by the filler becomes larger in the longitudinal (x_1) direction as ρ_β increases. As ρ_α becomes very large, α_{11}/α_m for the secondary aspect ratios approaches the limit for disc-shaped inclusions, as shown in Fig. 4. Fig. 5(b) shows that as ρ_α increases the CTE in the transverse direction, α_{22}/α_m, increases for the case of the fiber-shaped inclusions; however, it decreases for the case of disc-shaped particles. As ρ_β increases for a given ρ_α, α_{22}/α_m increases from the lower limit of disc-shaped inclusions to the upper limit of fiber-shaped particles. As ρ_α becomes very large, α_{22}/α_m converges to the limit of the disc-shaped inclusions like α_{11}/α_m. The CTE in the normal direction, α_{33}/α_m, increases as ρ_α increases for all secondary aspect ratios as shown in Fig. 5(c). As ρ_β increases for a given ρ_α, α_{33}/α_m decreases. At low ρ_α, the value of α_{33}/α_m can be slightly lower than predicted for fibers; however, as ρ_α becomes very large, the curves for any fixed ρ_β eventually approaches the disc-shaped limit. The bulk CTE ratio, $\gamma/3\alpha_m$, decreases as ρ_α increases for all given secondary aspect ratios as seen in Fig. 5(d). As ρ_β increases for a given ρ_α, $\gamma/3\alpha_m$ increases. At low ρ_α, the bulk coefficients for a given ρ_β may lie slightly above the fiber-shaped limit; but as ρ_α becomes very large, each curve for a given ρ_β approaches the disc-shaped limit. As seen in Figs. 2(d) and 5(d), $\gamma/3\alpha_m$ is much less influenced by addition of filler regardless of aspect ratios than the linear coefficients due to the compensating effects.

The effects of the secondary aspect ratio, ρ_β, on the various normalized CTEs are shown more directly in Fig. 6 by plotting the thermal expansion as a function of the secondary aspect ratio, ρ_β, for given primary aspect ratios, ρ_α, at a volume fraction of filler $\phi = 0.015$. The limits for spheres (the point where $\rho_\alpha = \rho_\beta = 1$), discs (the bold dotted line along which $\rho_\beta = 1$), and fibers (the bold line along which $\rho_\beta = \rho_\alpha$) are shown. In Fig. 6(a), α_{11}/α_m always decreases as ρ_β increases for a fixed ρ_α. In Fig. 6(b), as ρ_β increases for a fixed ρ_α, the transverse CTE α_{22}/α_m always increases in contrast to the behavior of α_{11}/α_m shown earlier. The CTE in the normal direction, α_{33}/α_m, decreases as ρ_β increases as shown in Fig. 6(c). For a fixed ρ_α, the bulk CTE, $\gamma/3\alpha_m$, generally increases as ρ_β increases and eventually merges with the curve for fiber-shaped particles as seen in Fig. 6(d).

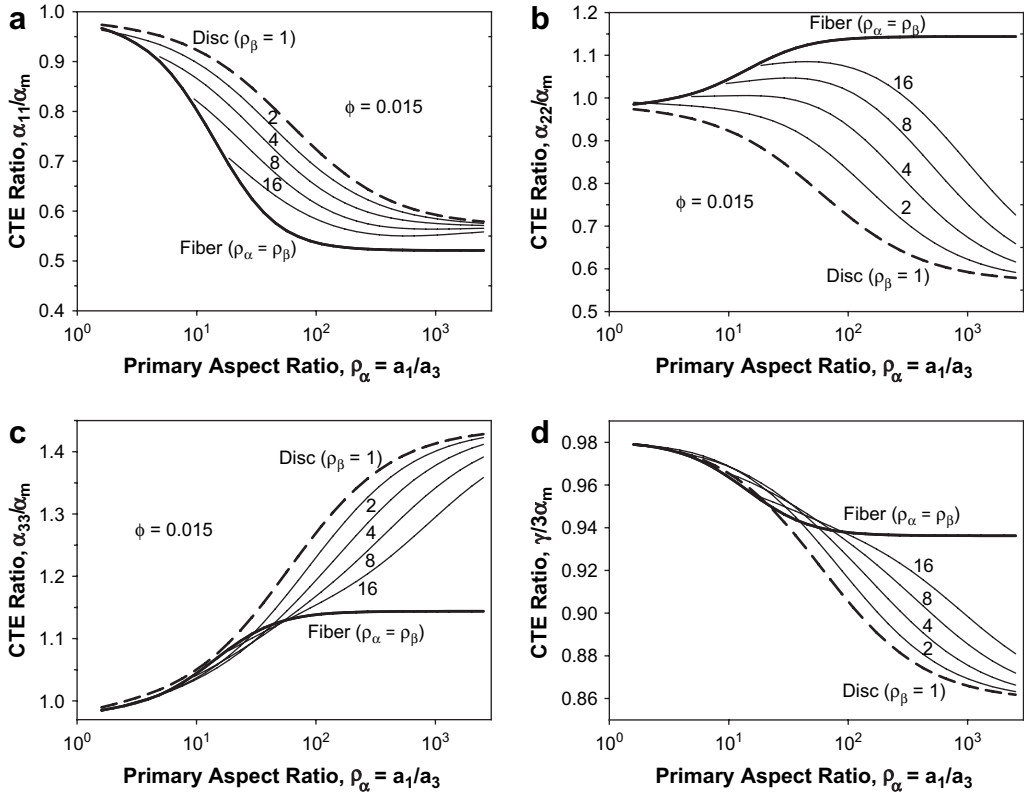

Fig. 5. Normalized coefficients of linear thermal expansion in the (a) longitudinal direction, α_{11}/α_m, in the (b) transverse direction, α_{22}/α_m, and in the (c) normal direction, α_{33}/α_m, and the (d) bulk coefficient of thermal expansion, $\gamma/3\alpha_m$, as a function of the primary aspect ratio ρ_α for a given volume fraction $\phi = 0.015$ and secondary aspect ratios of $\rho_\beta = 2$, 4, 8 and 16.

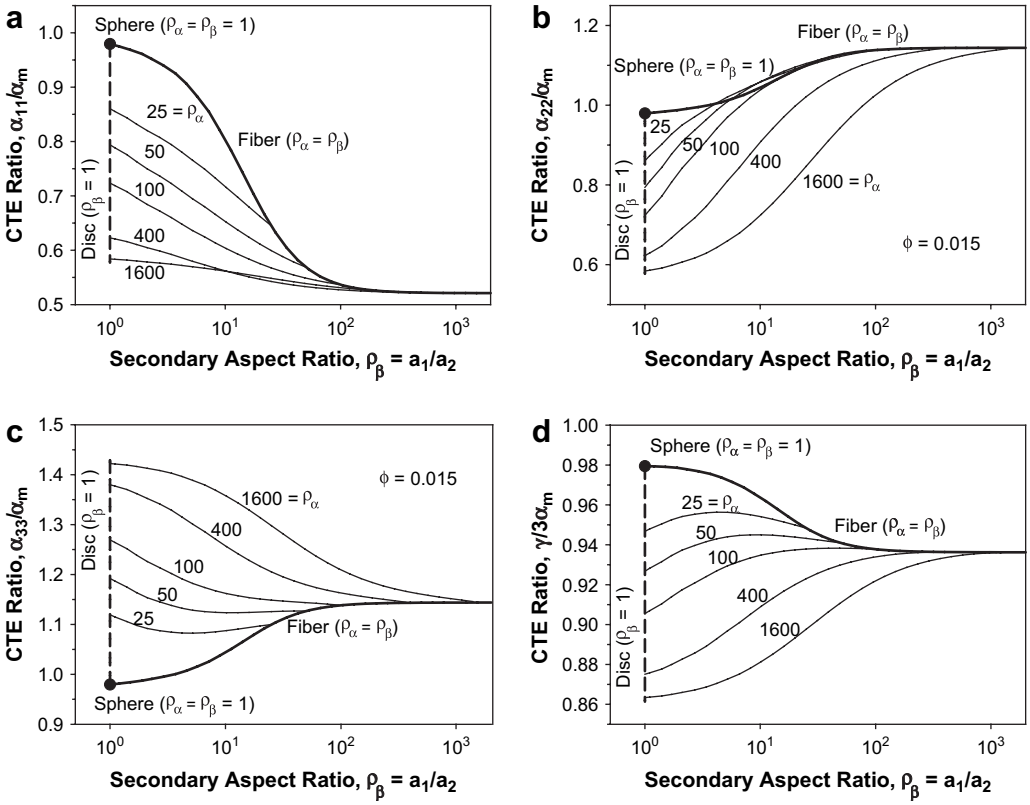

Fig. 6. Normalized coefficients of thermal expansion in the (a) longitudinal direction, α_{11}/α_m, in the (b) transverse direction, α_{22}/α_m, and in the (c) normal direction, α_{33}/α_m, and the (d) bulk coefficient of thermal expansion, $\gamma/3\alpha_m$, versus the secondary aspect ratio from $\rho_\beta = 1$ to $\rho_\beta = \rho_\alpha$ for fixed values of the primary aspect ratio from $\rho_\alpha = 25$ to $\rho_\alpha = 1600$ at a volume fraction of MMT filler of $\phi = 0.015$.

5. Conclusion

Using concepts described in prior papers [1,4], a model was developed here for calculating all three linear coefficients of thermal expansion, CTE, of composites based on aligned non-axisymmetric ellipsoids ($a_1 > a_2 > a_3$), characterized by two aspect ratios, ρ_α and ρ_β, as the inclusions. The basic model treats the case where the matrix polymer is anisotropic in its properties; however, matrix isotropy was assumed in all example calculations. The effects of the primary and secondary aspect ratios of the filler particles, over a filler volume fraction range of 0–6%, were illustrated by sample calculations for a matrix with properties of nylon 6 and a filler with the properties of single platelets of montmorillonite clay. In this example, the filler has considerably higher values of modulus and lower CTE than the polymer matrix.

The CTE in the longitudinal direction, α_{11}, of these composites decreases as the volume fraction of filler ϕ increases due to the constraint imposed by the inclusions. The CTE in the normal direction, α_{33}, increases as ϕ increases due to "squeezing" out of the matrix driven by the constraint in the longitudinal direction. The CTE in the transverse direction, α_{22}, is more complex and may increase or decrease with ϕ depending on the shape of the filler. The bulk or volumetric CTE, γ, is the sum of the three CTEs and always involves algebraically adding positive and negative changes with the result being that filler loading has much less effect on the volumetric thermal expansion than the case for the various linear coefficients of thermal expansion. At the low loadings used in nanocomposites, the various CTEs are rather similar to that of the matrix until the primary aspect ratio, ρ_α, exceeds about 10. The CTE reach limiting values when ρ_α becomes of the order of 10^3. As the secondary aspect ratio goes from $\rho_\beta = 1$ to $\rho_\beta = \rho_\alpha$, the model calculations show that CTE values in any coordinate direction go smoothly from the limit of a disc-shape ($\rho_\beta = 1$) to the limit of a fiber-shape ($\rho_\beta = \rho_\alpha$).

References

[1] Lee KY, Kim KH, Jeoung SK, Ju SI, Shim JH, Kim NH, et al. Polymer 2007;48:4174–83.
[2] Eshelby JD. Proc R Soc Lond 1957;A241:376–96.
[3] Mori T, Tanaka K. Acta Metall 1963;21:571–4.
[4] Lee KY, Paul DR. Polymer 2005;46:9064.
[5] Bowles D, Tompkins S. J Compos Mater 1989;23:370–88.
[6] Tandon GP, Weng GJ. Polym Compos 1984;5:327–33.
[7] Chow TS, Wilson JC. J Polym Sci Polym Phys Ed 1978;16:959–65.
[8] Chow TS. J Polym Sci Polym Phys Ed 1978;16:967–70.
[9] Chow TS. J Mater Sci 1980;15:1873–88.
[10] Yoon PJ, Fornes TD, Paul DR. Polymer 2002;43(25):6727–41.
[11] Hill RJ. Mech Phys Solid 1964;12:199–212.
[12] Halpin JC, Kardos JL. Polym Eng Sci 1976;16(5):344–52.
[13] Schapery RA. J Compos Mater 1968;2:380.
[14] Wakashima K, Otsuka M, Umekawa S. J Compos Mater 1974;8:391.
[15] Takao Y, Taya M. J Appl Mech 1985;52:806–10.
[16] Pierard O, Friebel C, Doghri I. Compos Sci Technol 2004;64:1587–603.
[17] Doghri I, Tinel L. Comput Methods Appl Mech Eng 2006;195:1387–406.
[18] Li J. Mech Mater 1999;31:149–59.
[19] Lusti H, Hine P, Gusev A. Compos Sci Technol 2002;62:1927–34.
[20] Dray D, Gilormini P, Regnier G. Compos Sci Technol 2007;67(7–8):1601–10.
[21] Hbaieb K, Wang Q, Chia Y, Cotterrell B. Polymer 2007;48:901–9.
[22] Glavchev I, Petrova K, Ivanova M. Polym Testing 2002;21(2):177–9.
[23] Alagar M, Ashok Kumar A, Mahesh KPO, Dinakaran K. Eur Polym J 2000;36(11):2449–54.
[24] Yalcin B, Cakmak M. Polymer 2004;45:6623–38.
[25] Fornes TD, Paul DR. Polymer 2003;44:3945–61.
[26] Fornes TD, Paul DR. Polymer 2003;44:4993–5013.
[27] Shah RK, Hunter DL, Paul DR. Polymer 2005;46:2646–62.
[28] Laura DM, Keskkula H, Barlow JW, Paul DR. Polymer 2003;44:3347–61.
[29] Ahn Y-C, Paul DR. Polymer 2006;47:2830–8.
[30] Lee H, Fasulo P, Rodgers W, Paul D. Polymer 2005;46(25):11673–89.
[31] Lee H, Fasulo P, Rodgers W, Paul D. Polymer 2006;47(10):3528–39.
[32] Ellis TS, D'Angelo JS. J Appl Polym Sci 2003;90:1639–47.
[33] Wei C, Srivastava D, Cho KJ. Nano Lett 2002;2(6):647–50.
[34] Zhang YC, Wang X. Int J Solid Struct 2005;42(20):5399–412.
[35] Carnahan B, Luther HA, Wilkes JO. Applied numerical methods. New York: John Wiley and Sons, Inc.; 1969.